

# Nanotechnology E-Newsletter

September 2005

## Enhanced photochemistry through optical cavity design

The fate of excited-state atoms or molecules in optical cavities is of particular interest due to the ability of the optical cavity to effect the radiative properties of the embedded atom or molecule.<sup>1</sup> Purcell's prediction that the rates of radiative processes are proportional to the optical density of states has been demonstrated with many optical resonator designs.<sup>2</sup>

Sandoghdar and coworkers, for example, demonstrated changes in the fluorescence lifetime of europium ions uniformly doped in silica spheres.<sup>3</sup> In their experiment, the fluorescence lifetime of individual spheres—with diameters ranging from 100nm to 2 $\mu$ m—was measured using a combination atomic force/confocal microscope. Their results confirmed predictions by Chew that dyes embedded in spheres smaller than the wavelength of light (sub-wavelength spheres) experience an overall inhibition in their radiative rate.<sup>4</sup> Furthermore, the effect of the spherical cavity on embedded dyes is rather independent of the radial position of the dye inside these sub-wavelength spheres. By comparison, the radial position has a dramatic effect on the radiative rate of a dye embedded in larger microspheres (i.e. whispering-gallery-mode resonators).

From a chemistry perspective, the ability to tune the rates of excited-state relaxation pathways is very appealing. For example, the quantum yield of a particular photochemical process is equal to the rate of the process divided by the sum of all competing rates. Thus, inhibition of fluorescence in sub-wavelength spheres could lead to enhanced quantum yields of electron- or energy-transfer reactions.

To demonstrate this concept, a ubiquitous

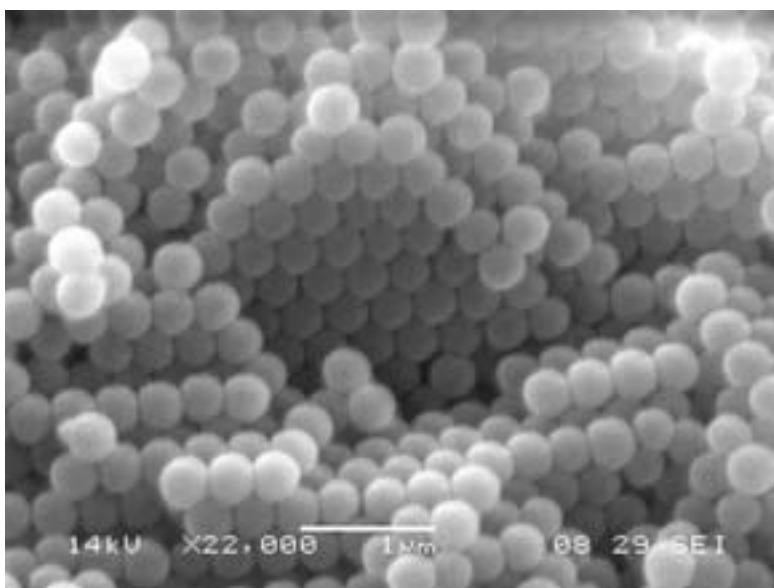


Figure 1. Typical silica spheres grown via the Stober process.

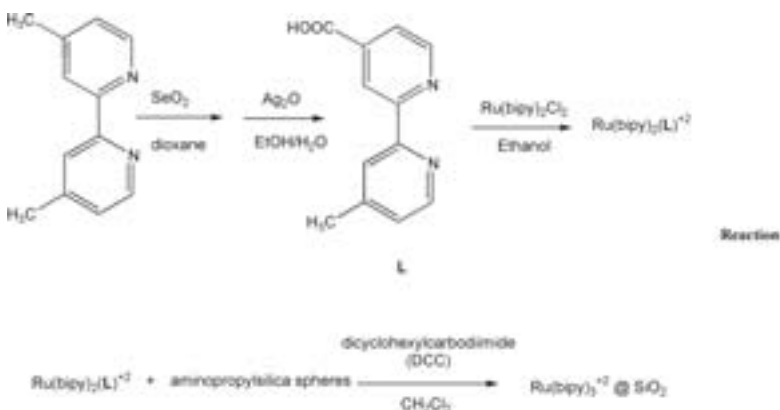


Figure 2. Reaction showing the acid-functionalized ruthenium dye covalently attached to the spheres via amide bond formation facilitated by dicyclohexylcarbodiimide (DCC).

photochemical ruthenium dye— $\text{Ru}(\text{bipy})_3\text{Cl}_2$ —was attached to various sub-wavelength spheres. The silica spheres used in our experiment were grown via the standard Stober method.<sup>5</sup> In this method, a tetraalkoxysilane (e.g. tetraethylorthosilicate, TEOS) is hydrolyzed under alkaline conditions to provide monodispersed spheres ranging in size from approximately 50-1000nm in diameter (see Figure 1). The spheres were then treated with aminopropyltriethoxysilane (APTES) to provide an amino functional group to which to attach a photochemical dye.  $\text{Ru}(\text{bipy})_3\text{Cl}_2$  was chosen as the dye due to its long excited-state lifetime and extensive photochemistry. The acid-functionalized ruthenium dye was covalently attached to the spheres via amide bond formation facilitated by dicyclohexylcarbodiimide (DCC, see Figure 2).

Typical fluorescence lifetime data shown in Figure 3 clearly suggests the decays are multi-exponential in nature and that the lifetime of the dye is inversely related to the sphere radius. It should be noted that we believe that there is some self-quenching between ruthenium centers.

We are currently varying the concentration of ruthenium centers to minimize this interaction and to simplify the decay curve.

To demonstrate enhanced photochemical

Continues on page 2.

## Enhanced photochemistry through optical cavity design

Continued from cover.

functionality, a Stern-Volmer quenching experiment was performed. For our preliminary quenching experiments, chromium (III) chloride in ethanol was used as the fluorescence quencher (see Figure 4). In this experiment, fluorescence of the dye decreases as quencher is added according to the Stern-Volmer relationship:  $I_0/I = k_q\tau_0[\text{quencher}] + 1$ . The proportionality constant is the product of the lifetime of the dye in the absence of quencher and the bimolecular quenching constant ( $k_q$ ). The enhanced slope for the 100nm spheres indicates more efficient quenching of the bound ruthenium than to both the free dye in solution and the dye bound to 500nm spheres.

A full theoretical treatment of the cavity effect is complicated by the multi-exponential decay rates and questionable position of the ruthenium dye, whether it is just under the surface or just above the surface of the silica sphere. We are currently attempting to resolve the multi-exponential decay issue by improving monodispersity of the spheres and optimizing the ruthenium doping level to prevent rapid self-quenching.

The authors wish to acknowledge the Research Corporation and DARPA Grant DAAD 19-03-1-0092 for funding of this project.

**Robert A. Hudgins, Adam Frake, G. F. Stout, Jasmine Gregory, and Thomas A. Schmedake**

Department of Chemistry and Center for Optics and Optoelectronics Communication  
University of North Carolina at Charlotte  
Charlotte, NC  
E-mail: tschmeda@email.uncc.edu

### References

1. K. J. Vahala, *Optical microcavities*, **Nature** **424** (6950), p. 839, 14 August 2003.
2. E. M. Purcell, *Spontaneous emission probabilities at radio frequencies*, **Physical Review** **69**, p. 681, 1946.
3. H. Schniepp and V. Sandoghdar, *Spontaneous emission of europium ions embedded in dielectric nanospheres*, **Phys. Rev. Lett.** **89** (25), 257403, 16 December 2002.
4. H. Chew, *Radiation and lifetimes of atoms inside dielectric particles*, **Physical Review A**, **38** (7), pp. 3410-3416, 1 October 1988.
5. W. Stober, A. Fink, and E. Bohn, *Controlled growth of monodisperse silica spheres in the micron size range*, **J. of Colloid and Interface Science** **26**, p. 62, 1968.

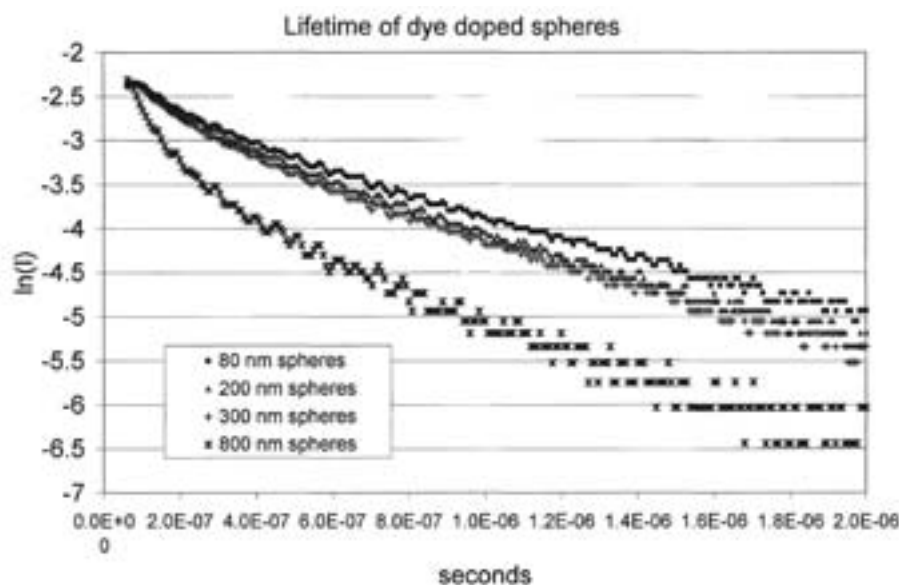


Figure 3. Fluorescence intensity decay of ruthenium-labeled spheres (natural log of intensity is shown).

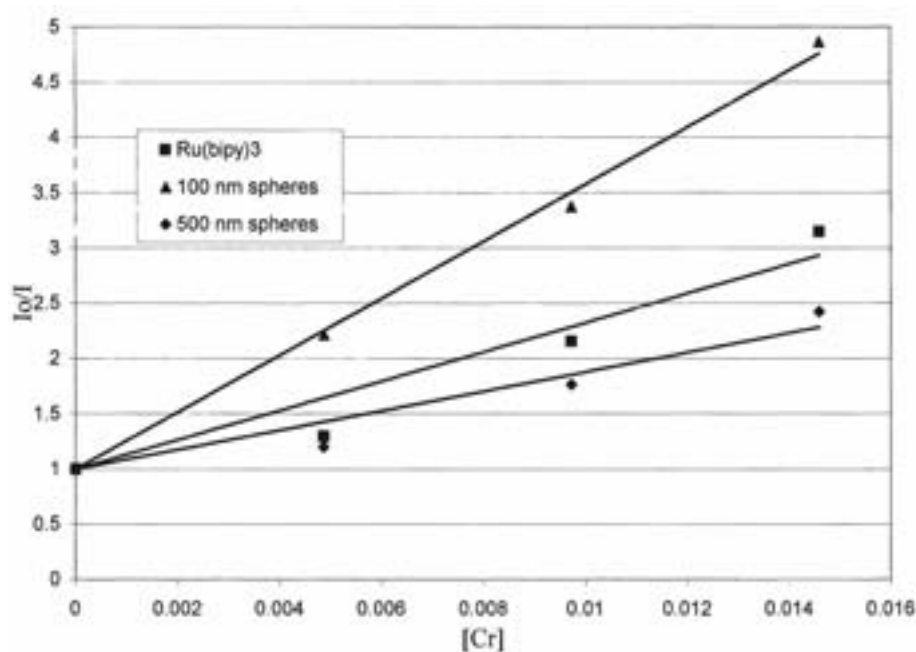


Figure 4. Stern-Volmer quenching experiment for spheres upon addition of chromium (III) chloride from 0 to 0.015 moles/L.

# Real-time observation of the docking of a single phage- $\lambda$ particle to its membrane receptor

Bacteriophages, viruses that infect bacteria, have recently been rediscovered as natural enhancers of mutagenesis, antibacterial therapeutic agents, and promising nanodevices. However, our knowledge of the complex molecular steps involved in phage infection is limited. We have chosen the phage- $\lambda$  paradigm as a means of dissecting the early stages of the infection process. Using high-resolution conductance recordings, we were able to track the docking of a single phage particle to its bacterial receptor: this gives us valuable clues towards understanding phage-host interactions.

Bacteriophages recognize their host via a 'key and lock' interaction with specific surface receptors. A trimeric channel-forming protein that mediates the bacterial consumption of maltooligosaccharides, maltoporin, had been identified as an outer-membrane docking site for phage  $\lambda$ : this is one of the best-known tailed phages. Previous studies of maltoporin interaction with the phage were addressed primarily by microbiological and biochemical methods, and via electron microscopy. Here, the phage was found to be able to attach to, and form stable complexes with, maltoporin *in vitro*.<sup>1</sup>

Functional properties of the maltoporin were studied via incorporation into planar lipid bilayers. Here, maltoporin forms stable trimeric ion-conductive channels that demonstrate pronounced sensitivity to the presence of maltose and maltodextrins.<sup>2</sup> Advanced conductance recording of the channel in the presence of solute permitted the detection of single sugar molecules translocating through the channel pores.<sup>3</sup> High-affinity interaction between the phage and maltoporin suggests that the binding process can modulate the transport characteristics of the ion-conductive channels.

We report here the real-time observation of phage  $\lambda$  docking to maltoporin at the single-particle level. In order to visualize the phage-receptor interaction we insert a single maltoporin trimer (purified from *E. coli* K12 pop154) into a planar lipid bilayer (for details see Reference 3) and studied its ion- and sugar-transport activity in the presence of the phage  $\lambda$  ( $\lambda$ cI ind<sub>857</sub> S<sub>sus7</sub>). With the high-resolution recordings we were able to detect the simultaneous and irreversible interaction of the phage tail with all three monomers of the maltoporin receptor.

Figure 1 shows four successive snapshots of current recordings from a single maltoporin tri-

mer in the presence of the phage  $\lambda$ . (A) Upon insertion into the bilayer, the maltoporin forms a stable channel with relatively-small steady ion conductance ( $\sim 200$ pS per trimer in 1M KCl). In the absence of sugars in the membrane-bathing solution, maltoporin exhibits a steady ion current. (B) Next, maltohexaose and phage were added to the solution on the 'extracellular' (*cis*-side) of the membrane. Maltohexaose (at 30 $\mu$ M concentration) creates vigorous fluctuations in the form of the stepwise reversible transitions to 2/3, 1/3, or (rarely) full blockage of the current through the trimer. These transitions correspond to transient retentions of single sugar molecules by the binding sites of the maltoporin pores.<sup>3,4</sup>

Within a time interval of 30-600s, (C) a phage particle docks to the trimer, reducing its ion current and entirely obstructing the sugar access to all three maltoporin pores: ion current through the receptor becomes steady again. (D) The addition of maltohexaose to the opposite ('periplasmic') side of the membrane (*trans*-side) causes characteristic stepwise current transitions, demonstrating that phage docking does not destroy the trimeric structure of the channel and its ability to interact with the substrate (maltohexaose). It also shows that, in the phage-attached configuration, transport properties of all three receptor monomers are modified in a similar way.

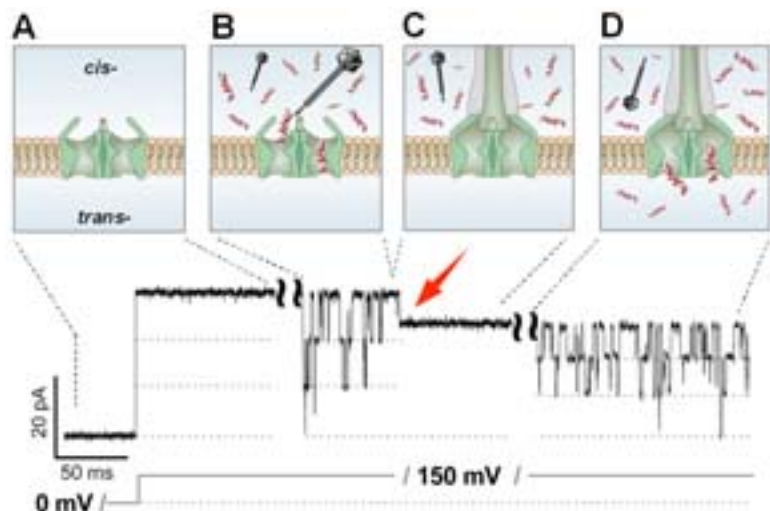


Figure 1. Current recording from a single maltoporin receptor inserted into a lipid bilayer permits detection of the attachment of a single phage particle. This is indicated by an abrupt shift in maltoporin transport properties (marked with arrow).

Philip A. Gurnev<sup>\*</sup>, Amos B. Oppenheim<sup>†</sup>, Mathias Winterhalter<sup>‡</sup>, and Sergey M. Bezrukov<sup>#</sup>

<sup>\*</sup>Laboratory of Physical and Structural Biology  
National Institute of Child Health and Human Development, Bethesda, MD

<sup>†</sup>Department of Molecular Genetics and Biotechnology

The Hebrew University, Hadassah Medical School, Israel

<sup>‡</sup>International University of Bremen, Bremen, Germany

<sup>#</sup>Corresponding author

E-mail: bezrukos@mail.nih.gov

## References

1. B. Dreiseikelmann, *Translocation of DNA across bacterial membranes*, **Microbiol. Rev.** **58** (3), pp. 293-316, September 1994.
2. R. Benz, A. Schmid, T. Nakae, and G. H. Vos-Scheperkeuter, *Pore formation by LamB of Escherichia coli in lipid bilayer membranes*, **J. Bacteriol.** **165** (3), pp. 978-986, March 1986.
3. L. Kullman, M. Winterhalter, and S. M. Bezrukov, *Transport of maltodextrins through maltoporin: a single-channel study*, **Biophys. J.** **82** (2), pp. 803-812, February 2002.
4. T. Schirmer, T. A. Keller, Y. F. Wang, and J. P. Rosenbusch, *Structural basis for sugar translocation through maltoporin channels at 3.1 Å resolution*, **Science**, **267** (5197), pp. 512-514, January 1995.

# An extension of microelectronic technology to nanoelectronics

The preparation of integrated circuits (ICs) on the 100Gbit integration scale (bits per die) may be possible with modest changes in current production process and marginal investment in fabrication facilities. We hypothesize an IC with a hybrid architecture: a standard silicon-based microelectronic section that controls a nanoscopic crossbar structure. At each cross point, the latter will host a collection of several (say,  $10^3$ - $10^4$ ) functional molecules, each able to mimic—by itself—the behavior of a flash memory cell. In this way, the hybrid circuit consists of a nanoscale kernel (carrying the memory elements) linked to a conventional submicron circuitry (for addressing, sensing, power supply, etc.).<sup>1</sup>

This architecture requires solutions to a number of problems. First is the set up of an economically-sustainable technology—i.e., one that does not involve excessive use of electron beam lithography (EBL)—for the preparation of  $10^{11}$  cross-points/cm<sup>2</sup>. In addition, a method of grafting the functional molecules to those cross-points must be found that uses some kind of batch processing. Next, some means of demultiplexing the address lines must be developed to allow their linkage to the microelectronic circuit. Finally, we must know how to design, synthesize, and electrically characterize the functional molecules.

All the above problems have been tackled in one way or another. Techniques for the preparation of arrays with pitch on the 10nm scale have been developed.<sup>1,2</sup> Hydrogen-terminated silicon can be functionalized using simple exposure to alkene-terminated molecules with the formation of chemically robust, environmentally stable, Si-C bonds.<sup>1</sup> Further, solutions have been found to the problem of demultiplexing,<sup>3</sup> and molecules admitting several conduction states are known.<sup>4</sup> Here, we review the status of solutions to the first problem.

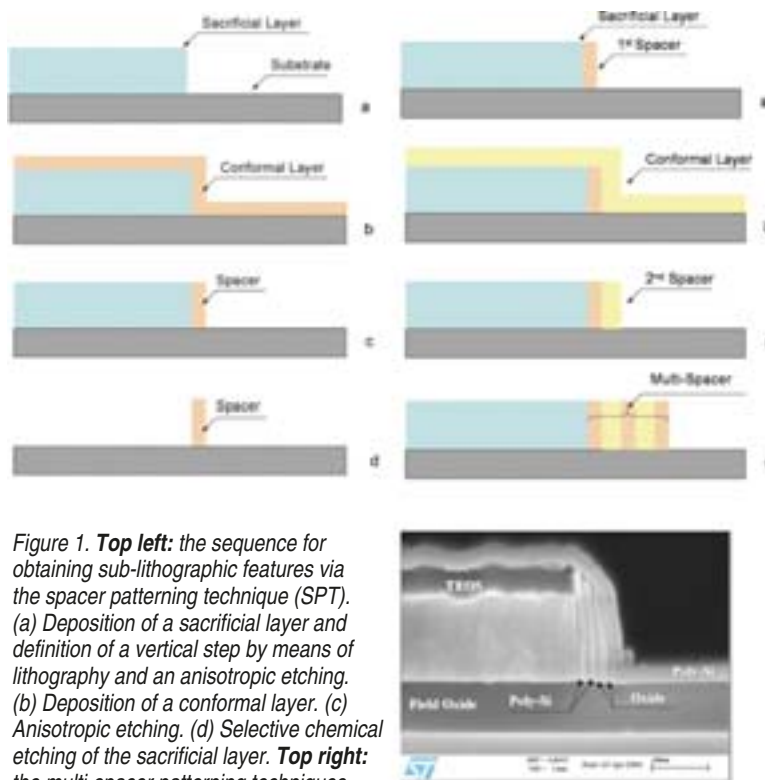


**Figure 1. Top left:** the sequence for obtaining sub-lithographic features via the spacer patterning technique (SPT). (a) Deposition of a sacrificial layer and definition of a vertical step by means of lithography and an anisotropic etching. (b) Deposition of a conformal layer. (c) Anisotropic etching. (d) Selective chemical etching of the sacrificial layer. **Top right:** the multi-spacer patterning techniques S<sup>N</sup>PT. (a) Fabrication of a first spacer by means of the SPT. (b) Deposition of a novel conformal layer. (c) Anisotropic etching and fabrication of a second array of another material. (d) Iteration of the sequence (b)-(c). **Bottom right:** an S<sup>3</sup>PT array resulting from three repetitions of the SPT process.

Arrays with pitch on the nanometer length scale (NLS) can be prepared by transforming vertical features (like the thickness of a film) into horizontal features. Although the producible geometries are essentially arrays, the minimum achievable pitch (10-20nm)<sup>1,2</sup> is considerably smaller than that currently achievable via electron-beam lithography (40-60nm). An example of the results achieved via the application of one of such techniques, the multispace patterning technique (S<sup>N</sup>PT), is sketched in Figure 1.

Being able to produce arrays with a pitch on the 10nm scale does not in itself allow the preparation of transistors with similar-sized features: transistor masks are more complex than simple arrays, and masks at different levels must have both definitions and alignments on

the NLS. Both these factors limit the scaling down of devices to the ultimate definition limit, but they disappear using the crossbar structure. Here, two perpendicularly-oriented arrays (orientation is not critical) are defined on two different levels, and each cross-point between the upper and lower arrays becomes the site containing the active molecular element.

The simplest way to prepare a crossbar circuit was first thought to be the following sequence: define the first-level array; deposit an active element (which will double as a vertical spacer); define the second-level array. This approach was used by a collaboration between Hewlett-Packard (HP) and the University of California at Los Angeles (UCLA) to prepare the kernel of a non-volatile memory.<sup>5</sup> However, this approach has a serious limit: the active organic element is incompatible with high-temperature processing, so the counter-electrode must be deposited at room temperature or slightly higher. This implies the need for physical vapor deposition, where the metallic electrode results from the

condensation of metal atoms on the outer surface of the organic film. Using this process has serious drawbacks in terms of compatibility, however: this is due to the high reactivity of the isolated metal atoms.<sup>6</sup>

Because we need to use organic chemistry to prepare molecules with the necessary electrical characteristics, the only way to overcome the difficulties met by the HP-UCLA collaboration seems the preparation of the two arrays defining the crossbar *before* the insertion of the molecule.<sup>7</sup> This would mean that a crossbar could be prepared via a sequence of two perpendicularly-oriented S<sup>N</sup>PTs and separated by an insulating NLS film: taking care to preserve the original film, or to regrow a film of equal thickness,<sup>1</sup> while fabricating the second S<sup>N</sup>PT. The intralayer oxide is finally etched selectively

*Continues on page 5.*

## An extension of microelectronic technology to nanoelectronics

Continued from page 4.

to form the hosting sites for the molecular guests. A simplified scheme is shown in the upper part of Figure 2.

This method has the additional advantage that its simplest implementation results in arrays of poly-silicon, whose surface can easily be functionalized with organic molecules.

The lower part of Figure 2 shows a cross section of a crossbar structure obtained with the S<sup>n</sup>PT using undoped poly-silicon and thermally-grown SiO<sub>2</sub>. This picture shows how two overlapped S<sup>n</sup>PTs, defined over an area of 350×350nm<sup>2</sup>, produce 49 cross points and a density of 4×10<sup>10</sup>cm<sup>-2</sup>.

### Gianfranco Cerofolini

STMMicroelectronics

Agrate, Italy

E-mail: gianfranco.cerofolini@st.com

### References

1. G. F. Cerofolini, G. Arena, M. Camalleri, C. Galati, S. Reina, L. Renna, and D. Mascolo, *A hybrid approach to nanoelectronics*, **Nanotechnology** **16**, pp. 1040-1047, 2005.
2. N. A. Melosh, A. Boukai, F. Diana, B. Gerardot, A. Badolato, P. M. Petroff, and J. R. Heath, *Ultrahigh-density nanowire lattices and circuits*, **Science** **300**, pp. 112-115, 2003.
3. A. DeHon, *Array-based architecture for FET-based, nanoscale electronics*, **IEEE Trans. Nanotechnol.** **2**, pp. 23-32, 2003.
4. C. P. Collier, E. W. Wong, M. Belohradsky, F. M. Raymo, J. F. Stoddart, P. J. Kuekes, R. S. Williams, and J. R. Heath, *Electronically configurable molecular-based logic gates*, **Science** **285**, pp. 391-394, 1999.
5. Y. Luo, C. P. Collier, J. O. Jeppesen, K. A. Nielsen, E. Delonno, G. Ho, J. Perkins, H. -R. Tseng, T. Yamamoto, J. F. Stoddart, and J. R. Heath, *Two-dimensional molecular electronics circuits*, **Chem. Phys. Chem.** **3**, pp. 519-525, 2002.
6. R. F. Service, *Next-generation technology hits an early midlife crisis*, **Science** **302**, pp. 556-559, 2003.
7. G. F. Cerofolini and G. Ferla, *Toward a hybrid micro-nanoelectronics*, **J. Nanoparticle Res.** **4**, pp. 185-191, 2002.

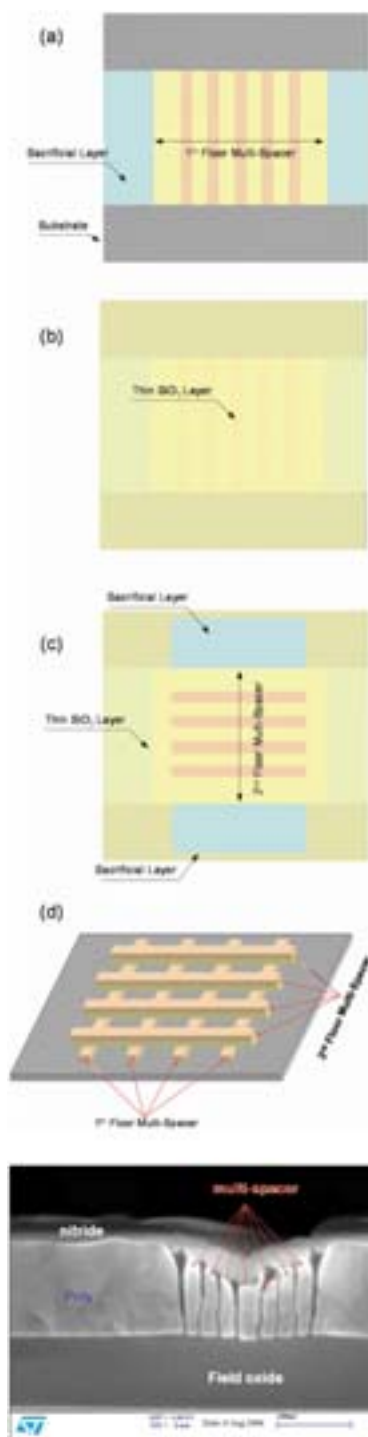


Figure 2. **Top:** crossbar fabrication steps. (a) Fabrication of a first-floor array of double spacers by means of S<sup>n</sup>PT. (b) Thermal growth of a thin film of SiO<sub>2</sub>. (c) Fabrication of a second-level array crossing the first-level array. (d) Selective chemical etching of the intralayer SiO<sub>2</sub>. **Bottom:** image at the scanning electron microscope of the cross section of a seven-spacer crossbar structure obtained with the S<sup>n</sup>PT process using undoped poly-silicon and thermally-grown SiO<sub>2</sub>.

# Hybrid plant-virus-inorganic nanostructures: assembly, characterization and applications

Fundamental limits on the scaling of semiconductor technology have motivated the search for new ways of fabricating nanoscale devices. A problem that has plagued many such techniques is size dispersion: it is extremely difficult to manufacture structures at the nanoscale that are functionally identical. Stress-driven assembly using molecular-beam epitaxy suffers from this problem: nanowires and quantum dots fabricated by conventional techniques vary significantly in size.

Recently, biological species, such as viruses, have been proposed as nanotemplates for the fabrication of nanoelectronic components.<sup>1,2</sup> Their natural advantage as nanotemplates lies in the fact that they are nearly identical in shape and size. Some plant viruses, such as *Tobacco mosaic virus* (TMV), are particularly suitable. TMV-U1 has a cylindrical

shape: this is convenient for fabricating nanowires, channels, and other nanocircuit elements. The rod-shaped virus has useful dimensions: it is 300nm long, 18nm in diameter, and has a 4nm axial channel. The availability of different variants of these viruses—characterized by their size, surface structure, genome sequence, and coat protein—expands the range of materials that can be produced via assembly. TMVs other advantages include their potential to form end-to-end assemblies, their selective attachment to predetermined locations, and their physical and chemical stability. In addition, TMVs can be coated with metals, silica, or semiconductors.

While using biological species as nanotemplates, the coating process must be monitored and the quality controlled. The adsorptivity and activity of metallic precursors with TMVs, and the speed of production, shape and location of reduced metals on the virus,

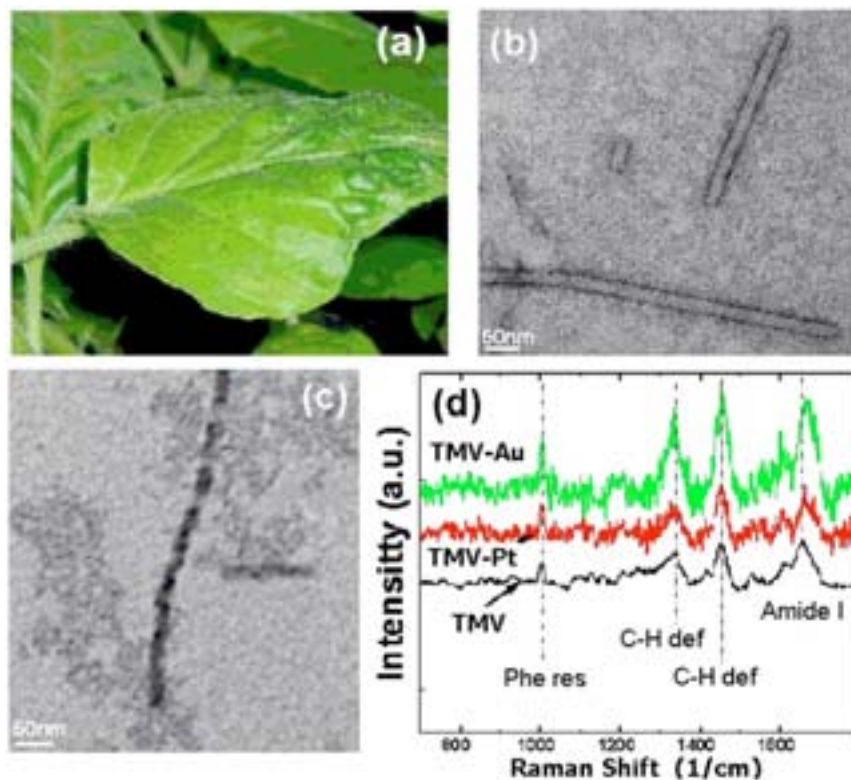


Figure 1. (a) Growth of Tobacco mosaic viruses (TMV) used as nano-templates. (b) TEM image showing a single 300nm TMV rod and an end-to-end, multi-particle TMV assembly. (c) TMV nano-assembly coated with Pt. (d) Raman spectra of native and coated TMVs.

are sensitive to the chemical environment, such as the buffer, pH and pK values, and so forth.

Our interdisciplinary team at the University of California at Riverside (UCR), which includes both electrical engineers and plant pathologists, has significantly improved on existing plant-virus nanotemplating methods. Further, we have proposed a new approach to characterizing the resulting hybrid plant-virus-inorganic nanostructures (details are reported elsewhere<sup>3</sup>). Using plant viruses as nanotemplates in this way the concepts of nanostructure growth and massively parallel production acquire entirely new meanings. Figure 1(a) shows *Nicotiana tabacum* 'Xanthi' plants inoculated with TMV-U1 in the UCR greenhouse. We inspected the formation and composition of the hybrid plant-virus-inorganic nanostructures using both transmission electron microscopy (TEM) and X-ray imaging; see Figure 1(b) and (c), where the single 300nm-long TMV

nanorods, end-to-end assembled aggregates, and Pt-coated TMV assembly are shown.

Water, the medium for the assembly process, is strongly infrared-absorbing. As a result, biological samples can generally be better studied using Raman rather than Fourier-transform infrared methods. Micro-Raman spectra of the native TMV, and of TMV coated with Pt and Au, are shown in Figure 1(d). Metal atoms attached to the TMV sidewall protein shell can change the TMV phonon signatures. The four most prominent peaks of pure TMV are the Amide I line at 1655cm<sup>-1</sup>, the C-H deformation lines at 1454.5cm<sup>-1</sup> and 1332cm<sup>-1</sup>, and the phenylalanine residue line at 1005cm<sup>-1</sup>. For TMV coated with Pt and Au, the most significant change in the Raman spectrum is that Amide I line shifts to 1664cm<sup>-1</sup> and 1672cm<sup>-1</sup>, respectively. Since the Amide I line is mainly a result of TMV coat-protein capsid, the apparent line shift indi-

icates the change of vibrational modes due to the binding of metal with a certain functional group in the shell protein. These results suggest that Raman spectroscopy can be used to detect the binding of the coating atoms with specific functional groups in the TMV particles.

Interpretation of Raman spectra and extraction of mechanical and structural information requires theoretical analysis of lattice vibrations in the hybrid nanostructures. Figure 2 shows the calculated vibrational frequencies and displacement fields for the first two radial modes of TMV in air.<sup>4</sup> The experimental and theoretical results obtained demonstrate that robust plant viruses, such as TMVs, are promising candidates for nanotechnology applications.

*The NDL group acknowledges program support of the MARCO FENA center.*

*Continues on page 7.*

## Hybrid plant-virus-inorganic nanostructures: assembly, characterization and applications

Continued from page 6.

A.A. Balandin<sup>#</sup>, W.L. Liu<sup>\*</sup>, K. Alim<sup>\*</sup>,  
V.A. Fonoberov<sup>\*</sup>, D.M. Mathews<sup>†</sup>, and J.A.  
Dodds<sup>†</sup>

<sup>\*</sup>Nano-Device Laboratory, Department of  
Electrical Engineering  
<http://ndl.ee.ucr.edu/>

<sup>†</sup>Department of Plant Pathology  
University of California, Riverside, CA

<sup>#</sup>Corresponding author  
E-mail: balandin@ee.ucr.edu

### References

1. W. Shenton, T. Douglas, M. Young, G. Stubbs, and S. Mann, *Inorganic-Organic Nanotube Composites from Template Mineralization of Tobacco Mosaic Virus*, *Adv. Mater.* **11**, pp. 253-256, 1999.
2. C. Mao, D. J. Solis, B. D. Reiss, S. T. Kottmann, R. Y. Sweeney, A. Hayhurst, G. Georgiou, B. Iverson, and A. M. Belcher, *Virus-Based Toolkit for the Directed Synthesis of Magnetic and Semiconducting Nanowires*, *Science* **303**, pp.213-217, 2004.
3. W. L. Liu, K. Alim, A. A. Balandin, D. M. Mathews, and J. A. Dodds, *Assembly and Characterization of Hybrid Virus-Inorganic Nanotubes*, *Appl. Phys. Lett.* **86** (25), p. 253108, 2005.
4. V. A. Fonoberov and A. A. Balandin, *Low-frequency vibrational modes of viruses used for nanoelectronic self-assembly*, *Phys. Stat. Sol. (b)* **241**, pp. R67-R69, 2004.

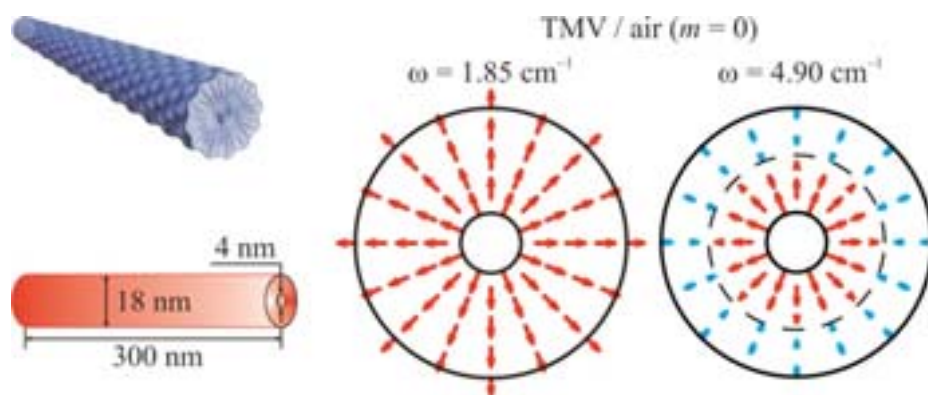


Figure 2. TMV schematic and radial vibrational modes for TMV in air. The direction and length of arrows correspond to the direction and magnitude of the displacement vector.

# Microlithography-free multi-valued analog memory device using self-assembled nanoparticle films

Digital computers use binary states, typically represented by 0 and 5V, to store and process information at all stages of a calculation. If more states, ideally a continuum, were available in between, the density of information could be dramatically increased. We have shown that self-assembled nanoparticle (NP) films can be used to implement this kind of continuous-state or analog information storage. Information is written in the film by trapping charges in a local, gate-modified potential, and is then read out using the film's built-in ability to sense charge via Coulomb blockade. Figure 1 is a schematic illustration of one of our devices.

To fabricate them, heavily-doped silicon chips were first annealed in oxygen to grow insulating oxides. The central trench is 1mm wide by 30nm thick, and the side oxides 2mm wide by 300nm thick: the thinner oxide in the trench results in an effective gate field. The whole oxide surface was derivatized with aminosilane (top left in Figure 1). The silane group sticks to the oxides, and the amino group to gold nanoparticles (~5nm in diameter), in this case synthesized in toluene by borohydride reduction.<sup>1,2</sup> The aminosilanized chip was alternately immersed in toluene solutions of gold NPs and butanedithiol (top right in Figure 1).<sup>1,2</sup> The dithiols link the gold NPs together. For our samples, a typical film resistance was on an order of 10M $\Omega$  after four NP/butanedithiol immersion cycles. Electrical contacts to NP films and to a bottom gate-Si were made with Indium. Self-assembly means our device fabrication process requires no microlithography, and therefore bridges between nanometer and micrometer length scales. In addition, layer-by-layer growth yields three-dimensional functional structures.

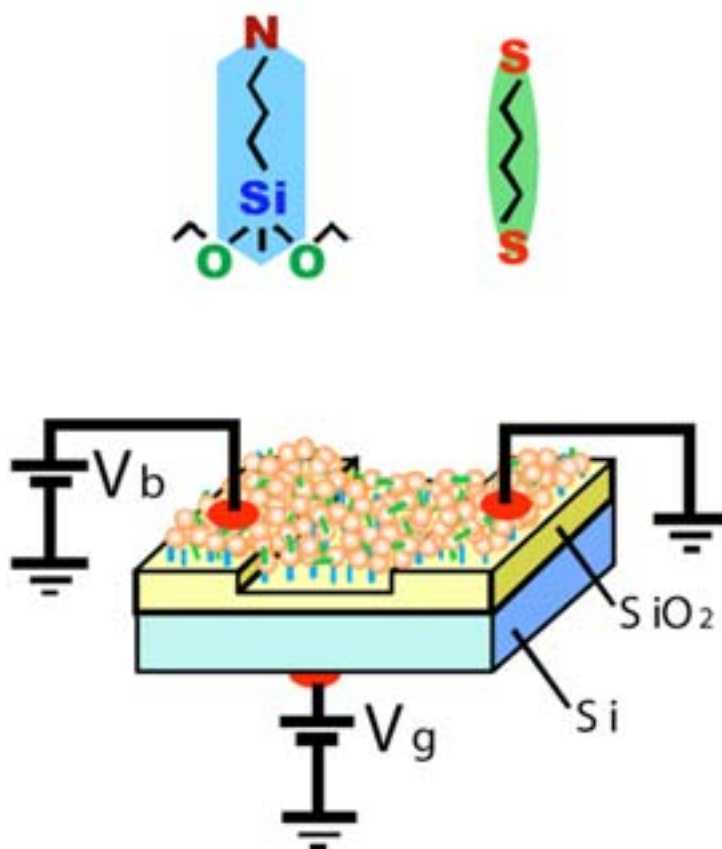


Figure 1. Schematic illustration of a nanoparticle (NP) device. Aminosilane (top left) and butanedithiol (top right) were used to form SiO<sub>2</sub>-NP and NP-NP linkages, respectively.  $V_b$  and  $V_g$  represent bias and gate voltages.

Figure 2(a) shows a typical differential conductance map measured at 77K as a function of bias and gate voltages ( $V_b$  and  $V_g$ ). We kept  $V_g=0$  during cooling from room temperature (RT). There is a conductance minimum near zero bias voltage at  $V_b=0$ , and the minimum moves in a diagonal direction as we vary  $V_g$ . Capacitance encountered along current pathways in the film present single-electron charging energy barriers and give rise to the minimum (Coulomb blockade<sup>3</sup>, CB) near  $V_b=0$  and  $V_g=0$ . Electrons have to overcome these energy barriers to flow through the film. The device can be used for conductance switching as in field effect transistors (FETs) since the charging energy barriers can be shifted by applying

$V_g$ , as observed in Figure 2(a).

Interestingly, this device 'remembers' values of gate voltages applied during cooling. We applied a two-valued square gate voltage shown in Figure 2(c) during cooling to 77K, and obtained the conductance map shown in Figure 2(b): two diagonal stripes can be seen in the conductance map. As shown in Figure 2(d), a cross-section through the center line in Figure 2(b) exhibits dips at  $V_g=-3V$  and  $+3V$ , which correspond to the two gate-voltage values applied during cooling. Since the choice of a two-valued square wave was arbitrary, this device can store multi-valued analog information by exploiting a continuum of choices for time-dependent gate voltages applied during cooling.

Figure 3 shows how this detailed information may be stored. We applied cyclic gate voltages (see middle of figure) to a device as it was cooled from RT to 77K, and wrote certain functions in the conductance map shown in the left and right. These functions, reading from  $V_g=5V$  towards  $-5V$ , resemble '· · · · ·' and '· ·' (U and T, respectively, in Morse code). The NP films can be used, in principle, to store any function,  $f(V_g)$ , using an appropriate series of  $V_g$  values and durations,  $\Delta t$ : this is because  $V_g$  and  $\Delta t$  can be used to set location and depth, respectively, of the CB minimum. Functions that can be stored are subjected to resolution constraints, and the magnitude of the maximum gate voltage depends on the robustness of the gate oxides. The latter can be increased so as to increase memory density.

Y. Suganuma and A. -A. Dhirani  
Department of Chemistry  
University of Toronto  
Toronto, Canada  
E-mail: adhirani@chem.utoronto.ca

Continues on page 9.



# Microlithography-free multi-valued analog memory device using self-assembled nanoparticle films

Continued from page 8.

### References

1. M. Brust, D. Bethell, C. J. Kiely, and D. J. Schiffrin, *Self-assembled Gold nanoparticle thin films with nonmetallic optical and electronic properties*, **Langmuir** **14** (19), p. 5425, 1998.
2. N. Fishelson, I. Shkrob, O. Lev, J. Gun, and A. D. Modestov, *Studies on charge transport in self-assembled Gold-dithiol films: conductivity, photoconductivity, and photoelectrochemical measurements*, **Langmuir** **17** (2), p. 403, 2001.
3. K. K. Likharev, *Correlated discrete transfer of single electrons in ultrasmall tunnel junctions*, **IBM J. Res. Develop.** **32** (1), p. 144, 1988.
4. Y. Suganuma, P.-E. Trudeau, and A. -A. Dhirani, *Multi-valued analogue information storage using self-assembled nanoparticle films*, **Nanotechnology** **16** (8), p. 1196, 2005.

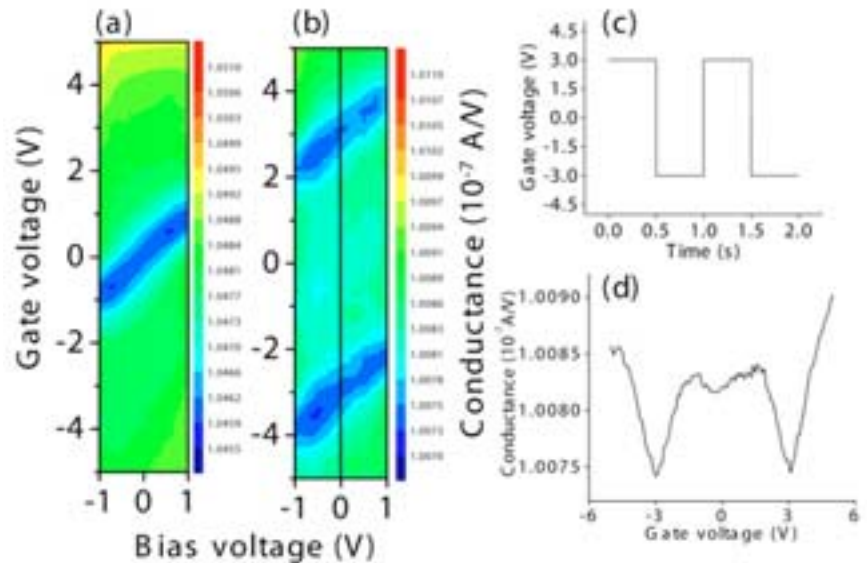


Figure 2. (a) A differential conductance map as a function of  $V_b$  and  $V_g$  obtained at 77 K and (b) after application of a square wave voltage (c) to  $V_g$  during cooling. (d) A cross-section of the conductance map through the centerline at  $V_b=0$  in (b).

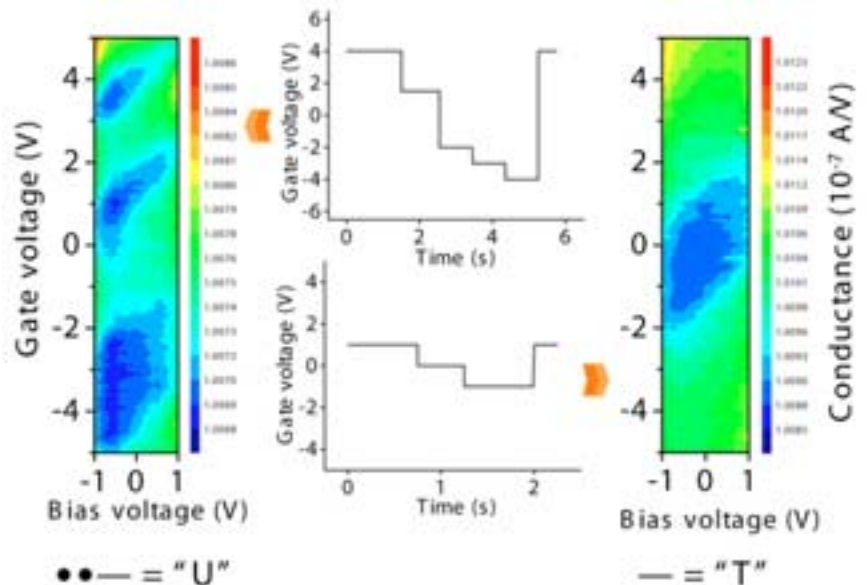


Figure 3. Differential conductance maps (left and right) obtained at 77K after cyclic 'writing' gate voltages (center) were applied during cooling from room temperature. The stored information in the conductance maps reading from  $V_g=5V$  to  $-5V$  were chosen to represent '· · ·' and '—': U and T in Morse code.

# Functionalized silicon membranes for filtration applications

Membranes with various pore size, length, morphology, and density have been synthesized out of various materials for size-exclusion-based separation. An example is the sterilization of intravenous lines by exclusion of bacteria and viruses using polyvinylidene fluoride membranes with 0.1 $\mu\text{m}$ -diameter pores. Chemically-specific filtration recently started to be addressed for small molecules<sup>1</sup> but specific bio-organism immobilization and detection remains a great technical challenge in many applications that require the analysis of samples such as air, drinking water, and body fluids.

The central goal of our research is to couple semiconductor nanotechnology and surface functionalization techniques in order to build sturdy platforms for the selective filtration of bio-organisms ranging in size from spores (many microns) down to viruses (tens of nanometers). The challenges of this research are threefold: to create channels with controlled position, length, and diameter ranging in size from many microns down to a few tens of nanometers; to localize the position of functional chemical units on these features; and—more than anything else—to control the organic/inorganic interface in confined geometries such as nano-channels.

Silicon constitutes a material of choice since its electronic properties and surface chemistry are well understood.<sup>2</sup> Advantage can be taken of this basic knowledge to both shape the material and chemically functionalize its surface.

Although a standard route to the chemical functionalization of silicon is to form an oxide layer and perform silane chemistry, some applications—such as the functionalization of luminescent silicon nanostructures—require defect-free surfaces. We have developed a synthetic route to covalently anchor bio-molecules to silicon starting with a hydride-terminated silicon surface. The surface is covalently functionalized with an amine-terminated chain using either a Lewis acid or light to catalyze the hydrosilylation reaction.<sup>3</sup> Protein cross-linker chemistry is then used to extend the linker and immobilize various molecules such as antibodies, proteins and live enzymes.<sup>4</sup>

We used light-assisted electrochemistry to

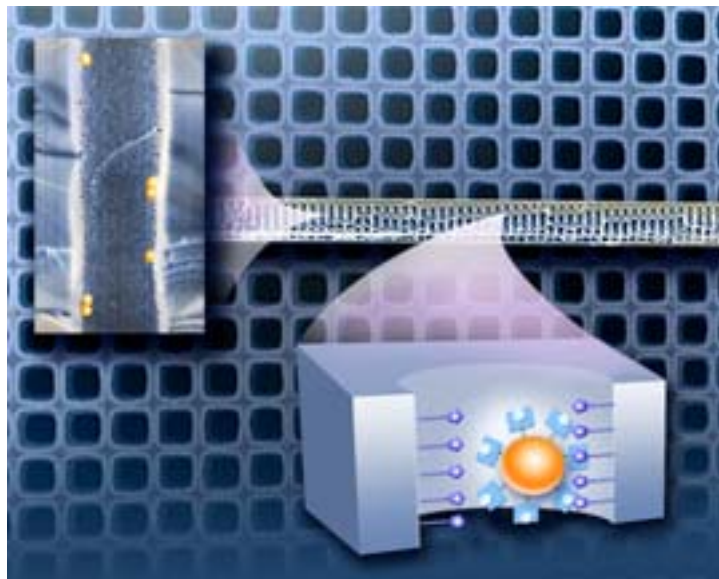


Figure 1. Top view (background), cross section (center) and zoom-out of a functionalized silicon membrane. These devices can be used to selectively capture simulated bio-organisms, colorized in orange.

produce periodic arrays of through pores on pre-patterned silicon membranes with controlled diameters ranging from many microns down to a few hundred nanometers.<sup>5</sup> We demonstrated the first covalently-functionalized silicon membranes and illustrated their selective capture abilities with antibody-coated fluorescent micro-beads simulating bio-organisms (see Figure 1). The antigen-functionalized membranes selectively captured the matching antibody-coated beads while allowing the rest of the beads to flow through. These engineered membranes are extremely versatile and could be adapted to specifically recognize the external fingerprints (size and membrane proteins) of any bio-organism of interest. A potential application is the pre-concentration of a specific organism for sample analysis. An example is the monitoring of *E. Coli* in recycled water produced by water-treatment plants.

By using breakdown electrochemical etching, we achieved periodic arrays with diameters down to 30nm and aspect ratios up to 250: numbers that had never been achieved previously using electrochemistry.<sup>6</sup> We demonstrated the potential of these devices for cell-encapsulation applications, for which the main challenge is to fabricate a capsule that allows the diffusion of glucose, a cell nutrient, while blocking

the diffusion of immunoglobulin, an antibody triggering foreign-body responses. An example of application is the encapsulation of pancreatic cells: the membrane can allow ions, glucose and insulin to move through while protecting the cells from foreign-body-response-triggering proteins.

Our next goal is to add *in situ* detection capabilities to the chemically-selective membranes. This would lead to a new class of platforms able to collect, concentrate, and analyze bio-organisms in real time. Applications for such a device are numerous, including counter-terrorism, human health and environmental monitoring.

*This work was performed under the auspices of the US Department of Energy by University of California Lawrence Livermore National Laboratory under contract number W-7405-Eng-48.*

## Sonia Létant

Chemistry and Materials Science  
Lawrence Livermore National Laboratory  
Livermore, CA  
E-mail: letant1@llnl.gov

## References

1. S. B. Lee, D. T. Mitchell, L. Trofin, T. K. Nevanen, H. Söderlund, and C. R. Martin, *Antibody-based bio-nanotube membranes for enantiomeric drug separation*, **Science** **296**, pp. 2198-2200, 2002.
2. J. M. Buriak, *Organometallic chemistry on silicon and germanium surfaces*, **Chem. Rev.** **102**, pp. 1271-1308, 2002.
3. B. R. Hart, S. E. Létant, S. R. Kane, M. Hadi, S. J. Shields, and J. G. Reynolds, *New method for attachment of biomolecules to porous silicon*, **Chemical Communications** **3**, pp. 322-323, 2003.
4. S. E. Létant, B. R. Hart, S. R. Kane, M. Hadi, S. J. Shields, and J. G. Reynolds, *Enzyme immobilization on porous silicon surfaces*, **Advanced Materials** **16**, pp. 689-693, 2004.
5. S. E. Létant, B. R. Hart, T. van Buuren, and L. J. Terminello, *Functionalized silicon membranes for bio-organisms capture*, **Nature Materials** **2**, pp. 391-395, 2003.
6. S. E. Létant, A. W. van Buuren, and L. J. Terminello, *Nanochannel arrays on silicon platforms by electrochemistry*, **Nano Lett.** **4**, pp. 1705-1707, 2004.

## Join the Nanotechnology Technical Group

**Please Print**     Prof.    Dr.    Mr.    Miss    Mrs.    Ms.

First Name, Middle Initial, Last Name \_\_\_\_\_

Position \_\_\_\_\_ SPIE Member Number \_\_\_\_\_

Business Affiliation \_\_\_\_\_

Dept./Bldg./Mail Stop/etc. \_\_\_\_\_

Street Address or P.O. Box \_\_\_\_\_

City/State \_\_\_\_\_ Zip/Postal Code \_\_\_\_\_ Country \_\_\_\_\_

Telephone \_\_\_\_\_ Telefax \_\_\_\_\_

E-mail Address/Network \_\_\_\_\_

**Technical Group Membership fee is \$30/year, or \$15/year for full SPIE members.**

Nanotechnology  
**Total amount enclosed for Technical Group membership**                      \$ \_\_\_\_\_

**Check enclosed.** Payment in U.S. dollars (by draft on a U.S. bank, or international money order) is required. Do not send currency. Transfers from banks must include a copy of the transfer order.

**Charge to my:**    VISA    MasterCard    American Express    Diners Club    Discover

Account # \_\_\_\_\_ Expiration date \_\_\_\_\_

Signature \_\_\_\_\_  
(required for credit card orders)

**E**xpand the area and scope of your knowledge by connecting directly with others in your field. SPIE Technical Groups bring colleagues together to communicate new ideas, approaches, and challenges, not just in one country or once a year, but all over the world, all the time.

As a technical group member you will:

- Keep pace with rapid change through focused information from SPIE.
- Gain contacts in your industry with an online membership directory.
- Network with colleagues at conferences and special events.
- Influence future technical activities within SPIE.

Prepare for what's next in your field and in your career. Join today!

**SPIE • P.O. Box 10  
 Bellingham, WA 98227-0010 USA  
 Tel: +1 360 676 3290  
 Fax: +1 360 647 1445  
 E-mail: [spie@spie.org](mailto:spie@spie.org)**

**Please send me**

- Information about SPIE Membership  
 Information about other SPIE technical groups  
 FREE technical publications catalog

**Reference Code: 4171**

## Nanotechnology

This e-newsletter is published quarterly by SPIE—The International Society for Optical Engineering.

|                            |             |                         |               |
|----------------------------|-------------|-------------------------|---------------|
| <i>Editor</i>              | Sunny Bains | <i>Managing Editor</i>  | Rich Donnelly |
| <i>Editorial Assistant</i> | Stuart Barr | <i>Graphic Designer</i> | Linda DeLano  |

*Editorial Board Members:*

**David Andrews**, Univ. of East Anglia; **James Grote**, Air Force Research Lab; **Jonathon Howard**, Max Planck Institute and Univ. of Washington; **Laszlo Kish**, Texas A&M University; **Akhlesh Lakhtakia**, Pennsylvania State Univ.; **Christi Madsen**, Bell Labs, Lucent Technologies; **Nils Peterson**, Nat'l Inst. for Nanotechnology, Univ. of Alberta; **Paras Prasad**, State Univ. of NY at Buffalo; **Mike Sailor**, Univ. of California at San Diego; **Richard Silver**, National Institute of Standards

Articles in this newsletter do not necessarily constitute endorsement or the opinions of the editors or SPIE.

SPIE is an international technical society dedicated to advancing engineering, scientific, and commercial applications of optical, photonic, imaging, electronic, and optoelectronic technologies. Its members are engineers, scientists, and users interested in the development and reduction to practice of these technologies. SPIE provides the means for communicating new developments and applications information to the engineering, scientific, and user communities through its publications, symposia, education programs, and online electronic information services.

Copyright ©2005 Society of Photo-Optical Instrumentation Engineers. All rights reserved.

**SPIE—The International Society for Optical Engineering**, P.O. Box 10, Bellingham, WA 98227-0010 USA.  
 Tel: +1 360 676 3290. Fax: +1 360 647 1445.

**European Office:** Karin Burger, Manager, [karin@spieurope.org](mailto:karin@spieurope.org), Tel: +44 7974 214542. Fax: +44 29 2040 4873.

**In Russia/FSU:** 12, Mokhovaja str., 119019, Moscow, Russia • Tel/Fax: +7 095 202 1079  
 E-mail: [edmund.spierus@relcom.ru](mailto:edmund.spierus@relcom.ru)